Abstract for the 29th Intl Workshop on Water Waves and Floating Bodies, Osaka (Japan), March 30 – April 02, 2014

Experimental Confirmation of Reciprocity Relations of Waves around an Asymmetric Floating Body

by Masashi Kashiwagi* and Takafumi Hayashi
Research Institute for Applied Mechanics, Kyushu University, Fukuoka, Japan
E-mail: *kashi@riam.kyushu-u.ac.jp*

Highlights:

- With Green's theorem, reciprocity relations are newly found for the waves around an asymmetric floating body freely oscillating in waves. Correctness of those relations are confirmed by numerical computations.
- 2-D experiments are conducted to confirm the theory, measuring the reflected and transmitted waves, and a pratical correction method for attenuation of the reflection wave is proposed.

1. Introduction

For the development of efficient floating breakwaters, a large number of theoretical studies have been made so far. As a consequence, particularly for a symmetric floating body, some important properties of the reflection and transmission waves are known [1]. On the other hand, for an asymmetric floating body, Bessho [2] proved for the diffraction problem that (1) both amplitude and phase of the transmission wave are the same and (2) the amplitude of the reflection wave is the same, irrespective of the incoming direction of incident wave.

Recently, by using Green's theorem, Kashiwagi [3] has proved that the properties of (1) and (2) for a fixed asymmetric body are also true even when the body is oscillating in an incident wave. These properties were also confirmed in numerical computations using the wave Green-function method.

However, in real flows, since the energy dissipation due to the viscosity of fluid must exist, the properties proved on the assumption of potential flow may not be satisfied. Therefore, in this study, we are carrying out 2-D experiments using an asymmetric body to confirm how much the relations proved theoretically are satisfied in a real fluid of water. In the experiment, the incident wave and reflection wave must be separated from the temporal wave data measured at some upwave points of a body. This paper describes a device in the measurement for achieving that purpose and a correction method for taking account of the decay of progressive wave in a 2-D wave channel.

2. Review of Reflection and Transmission Waves

The potential flow around a 2-D asymmetric floating body in regular incident waves is considered The wave-induced motion of a body and associated fluid motion are assumed to be linear in the incident-wave amplitude and harmonic in time with circular frequency ω of the incident wave. In what follows, all oscillatory quantities will be expressed in complex form, with the time dependence $e^{i\omega t}$ understood.

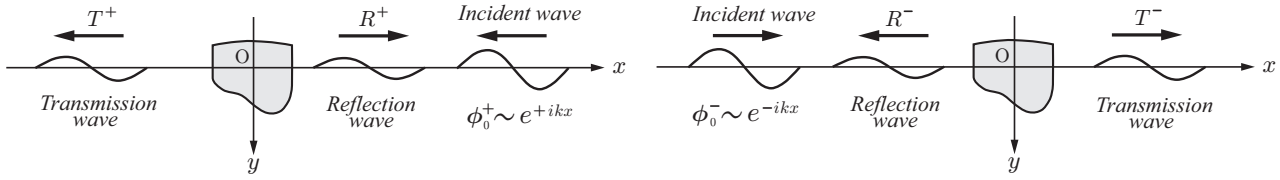

Fig. 1 Reflection and transmission waves for a 'positive' incident wave incoming from the positive x-axis (left figure) and for a 'negative' incident wave incoming from the negative x-axis (right figure).

Let us consider first the case of 'positive' incident wave (see the left in Fig. 1). Then the asymptotic expression of the normalized velocity potential at $x \to \pm\infty$ and $y = 0$ may be written as follows:

$$\varphi^+(x,0) \sim \begin{cases} e^{ikx} + R_F^+ e^{-ikx} & \text{as } x \to +\infty \\ T_F^+ e^{ikx} & \text{as } x \to -\infty \end{cases} \tag{1}$$

where

$$\left.\begin{aligned} R_F^+ &= R_D^+ - iKX_j^+ H_j^+, \quad R_D^+ = iH_4^+ \\ T_F^+ &= T_D^+ - iKX_j^+ H_j^-, \quad T_D^+ = 1 + iH_4^- \end{aligned}\right\} \tag{2}$$

Here k is the wavenumber satisfying the dispersion relation of $k\tanh kh = \omega^2/g \equiv K$, with h being water depth and g gravitational acceleration. X_j^+ denotes the complex amplitude of the wave motion in the j-th mode ($j = 1$ for sway, $j = 2$ for heave, and $j = 3$ for roll). $H_j^{\pm}$ ($j = 1 \sim 3$) and $H_4^{\pm}$ denote the Kochin functions associated with the far-field radiated and scattered waves, respectively. R^+ and T^+ are defined as the coefficients of reflection and transmission waves, respectively. Suffix D to these coefficients indicates the quantities for the diffraction problem; likewise suffix F indicates the quantities for the case where a body is freely oscillating in an incident wave.

Second, as shown on the right of Fig. 1, we consider the case of 'negative' incident wave. In this case, the asymptotic expression of the normalized velocity potential at $x \to \pm\infty$ and $y = 0$ may be written in the form

$$\varphi^-(x,0) \sim \begin{cases} T_F^- e^{-ikx} & \text{as } x \to +\infty \\ e^{-ikx} + R_F^- e^{ikx} & \text{as } x \to -\infty \end{cases} \tag{3}$$

where

$$\left.\begin{aligned} R_F^- &= R_D^- - iKX_j^- H_j^-\,, \quad R_D^- = ih_4^- \\ T_F^- &= T_D^- - iKX_j^- H_j^+\,, \quad T_D^- = 1 + ih_4^+ \end{aligned}\right\} \tag{4}$$

With preparation above, we consider Green's theorem, which gives the following equation:

$$\int_{S_H} \left(\phi\frac{\partial\psi}{\partial n} - \psi\frac{\partial\phi}{\partial n}\right) d\ell = \frac{K + h(k^2 - K^2)}{2k^2}\left[\left(\phi\frac{\partial\psi}{\partial x} - \psi\frac{\partial\phi}{\partial x}\right)_{y=0}\right]_{-\infty}^{+\infty} \tag{5}$$

Here both potentials ϕ and ψ are assumed to satisfy the same boundary conditions on the free surface and water bottom, but not necessarily the same boundary conditions on the body surface (S_H) and the radiation surface at $x = \pm\infty$. The square brackets with superscript $+\infty$ and subscript $-\infty$ means the difference between the quantities in the brackets evaluated at $x = +\infty$ and $x = -\infty$.

Considering φ^+ for ϕ and φ^- for ψ, we can prove the first important relation:

$$T_F^+ = T_F^-\,. \tag{6}$$

This means that the transmission wave past an asymmetric body freely oscillating in an incident wave is independent of the incoming direction of incident wave and must be the same in both amplitude and phase.

Next, considering $\overline{\varphi^+}$ (complex conjugate of φ^+) for ϕ and φ^- for ψ, the following relation can be obtained:

$$R_F^-\,\overline{T_F^+} + \overline{R_F^+}\,T_F^- = 0\,. \tag{7}$$

Combining (6) with (7) tells us another important relation that the amplitude of the reflection wave must be the same irrespective of the incoming direction of incident wave, but the phase is different depending on the incoming direction of incident wave.

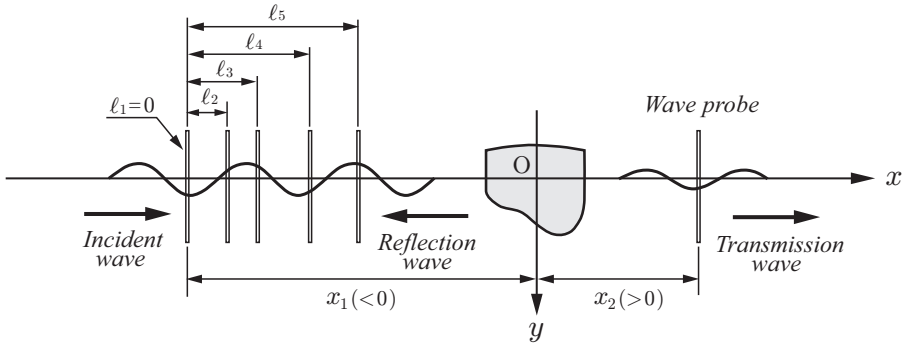

Fig. 2 Position of wave probes and associated notations.

3. Analysis Method in Experiment

The time history of the wave to be measured at a location between the wavemaker and a body includes both incident wave and reflection wave. In order to separate these, as Goda *et al.* [4] proposed, we must measure the wave at least at two different positions with certain distance at the same time. For enhancing the accuracy and reliability in the experiment analysis, we propose a new method using the plural number (N) of wave probes and the least-squares method with simultaneous measurements of the wave at N (> 2) different positions. As shown in Fig. 2, the wave probe located farthest from the body is denoted as No. 1 and its position is $x = x_1$ (< 0). Similarly the position of the j-th wave probe is denoted as $x_j = x_1 + \ell_j$ ($j = 1 \sim N$), where ℓ_j is defined positive and $\ell_1 = 0$.

Let us express the incident wave (ζ_I) and the reflection wave (ζ_R) in the following form:

$$\left.\begin{aligned}\zeta_I &= a_I \cos(\omega t - kx + \theta_I)\\ \zeta_R &= a_R \cos(\omega t + kx + \theta_R)\end{aligned}\right\} \tag{8}$$

where (a_I, θ_I) and (a_R, θ_R) are the amplitude and phase of the incident wave and the reflection wave, respectively; these are to be determined from the measurement.

The time history of the wave measured at the j-th position will be decomposed with the Fourier series, and let us write the first harmonic component as

$$\zeta_j = (\zeta_I + \zeta_R)_{x=x_j} \equiv A_j \cos\omega t + B_j \sin\omega t \quad (j = 1 \sim N) \tag{9}$$

From (8) and (9), it follows that

$$A_j = \alpha_C \cos(k\ell_j) - \alpha_S \sin(k\ell_j) + \beta_C \cos(k\ell_j) - \beta_S \sin(k\ell_j) \tag{10}$$

$$B_j = \alpha_C \sin(k\ell_j) + \alpha_S \cos(k\ell_j) - \beta_C \sin(k\ell_j) - \beta_S \cos(k\ell_j) \tag{11}$$

where

$$\left.\begin{aligned}\alpha_C &= a_I \cos\phi_I, \quad \alpha_S = a_I \sin\phi_I, \quad \phi_I = kx_1 - \theta_I\\ \beta_C &= a_R \cos\phi_R, \quad \beta_S = a_R \sin\phi_R, \quad \phi_R = kx_1 + \theta_R\end{aligned}\right\} \tag{12}$$

Applying the least-squares method to (10) and (11), unknown coefficients $\alpha_C, \alpha_S, \beta_C$, and β_S may be determined. Then (a_I, θ_I) and (a_R, θ_R) can be determined from (12), and the final results can be expressed with the incident wave taken as the phase reference, as follows:

$$\left.\begin{aligned}\zeta_I &= a_I \cos(\omega t - kx)\\ \zeta_R &= a_R \cos(\omega t + kx + \delta_R)\end{aligned}\right\} \tag{13}$$

where

$$\left.\begin{aligned}a_I &= \sqrt{\alpha_C^2 + \alpha_S^2}\,, \; a_R = \sqrt{\beta_C^2 + \beta_S^2}\\ \delta_R &= -2kx_1 + \tan^{-1}(\beta_S/\beta_C) + \tan^{-1}(\alpha_S/\alpha_C)\end{aligned}\right\} \tag{14}$$

The transmission wave can be determined from the measurement at a downwave position, denoted as $x = x_2$ (> 0), of which the analysis method using the Fourier series is well-established and thus its explanation is omitted here. We should note that the case of $N = 2$ in the above procedure retrieves the Goda's result [4].

4. Tested Model and Interim Results

The experiment is carried out in the wave channel (10 m in length, 0.4 m in water depth, and 0.3 m in width) at RIAM, Kyushu University, with an asymmetric body shown in Fig. 3; each of the right and left section shapes below the still water line is of Lewis form that can be represented by a conformal mapping in terms of the half breadth-to-draft ratio $H_0 = b/d$ and the sectional area ratio $\sigma = S/bd$. As shown in Fig. 3, the right-hand shape ($x > 0$) is for $H_0 = 1.0$ and $\sigma = 0.95$ and the left-hand shape ($x < 0$) is for $H_0 = 1.0$ and $\sigma = 0.60$.

Because there were some problems in the experimental set-up and we needed much time for identifying attenuation of the wave amplitude while the wave propagating in the wave channel, only the results for the diffraction problem can be reported in this paper. Remaining results may be presented at the Workshop.

Figure 4 shows the results of the reflection and transmission wave coefficients for both cases of the positive and negative incident waves. No correction is made for taking account of the wave attenuation during the propagation along the wave channel. First of all, we can see that the reciprocity relations, that is, $\left|T_F^+\right| = \left|T_F^-\right|$ and $\left|R_F^+\right| = \left|R_F^-\right|$, are satisfied with good accuracy in the measured results. However, prominent discrepancy exists in the magnitude of the reflection-wave coefficient between measured and computed results, implying obviously dissatisfaction of the wave-energy conservation.

We noticed attenuation of the wave amplitude through the measurement of incident waves only. Therefore, in order to obtain a correction coefficient associated with attenuation of the wave amplitude, we conducted a subsidiary experiment using a vertical wall that reflects the incident wave completely. Figure 5 shows the results, in which the reflection-wave coefficient is obviously smaller that 1.0 to be expected at all frequencies tested. With an assumption that both incident wave and reflection wave decay in proportion to the propagation distance, the following relation

$$(R)_e(\,1 - \alpha\ell_a\,)^2 = (R)_m \tag{15}$$

$$\frac{(R)_m}{(\,1 - \alpha\ell_a\,)^2} = (R)_e = 1.0 \tag{16}$$

$$\alpha = \frac{1}{\ell_a}\Big\{\,1 - \sqrt{(R)_m}\Big\} \tag{17}$$

were applied to obtain the attenuation factor α, where $(R)_e$ and $(R)_m$ denote respectively expected and measured values of the reflection-wave coefficient, and ℓ_a is the average distance of the measured points up to the vertical wall. After determining the value of α with $(R)_e = 1.0$ specified at all frequencies tested, the results shown in Fig. 4 were corrected in terms of the following equations:

$$R = \frac{(R)_m}{(1-\alpha\ell_a)^2}\,, \quad T = \frac{(T)_m}{(1-\alpha\ell_a)(1-\alpha\ell_T)} \tag{18}$$

Here $\ell_T\ (= x_2)$ denotes the position of the wave probe for measuring the transmission wave. The results after correction based on (18) are shown in Fig. 6, and we can see that the degree of agreement particularly in the reflection wave coefficient is much improved. Nevertheless, we can see that the conservation of wave energy is still not satisfied; this may be attributed partly to the energy dissipation around a body due to the viscosity of fluid. Subsequent experiments are still ongoing for checking the conservation of wave energy, the phase difference, and for the case where a body oscillates in waves which is the original purpose of the present experiment.

References

[1] Bessho, M. 1965, On the Theory of Rolling Motion of Ships among Waves, *Report of Scientific Research of Defence Academy*, Vol. 3, No. 1, pp. 47–59.

[2] Bessho, M. 1975, On Time-Reversed Velocity Potentials in the Theory of Water Waves, *J. Kansai Society of Naval Architects*, No. 159, pp. 75–84.

[3] Kashiwagi, M. 2006, Wave Reflection and Transmission by an Asymmetric Floating Body in Regular Waves, *Proceedings of 2nd PAAMES and AMEC2006* (Jeju, Korea), pp. 50–60.

[4] Goda, Y., Suzuki, Y. et al. 1976, A Method for Separating Incident and Reflected Waves in Experiment with Irregular Waves, *Technical Note of the Port and Airport Research Institute*, No. 248, pp. 3–24.

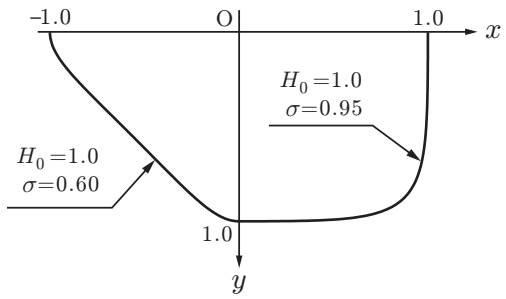

Fig. 3 Section shape of asymmetric Lewis-form body used in the experiment and numerical computations.

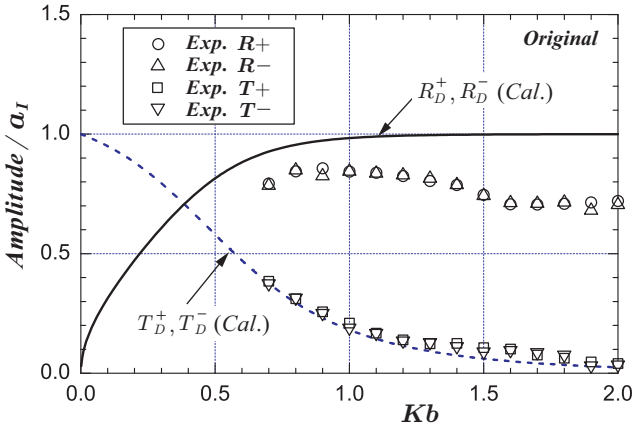

Fig. 4 Reflection and transmission coefficients for the diffraction problem (original data with no correction).

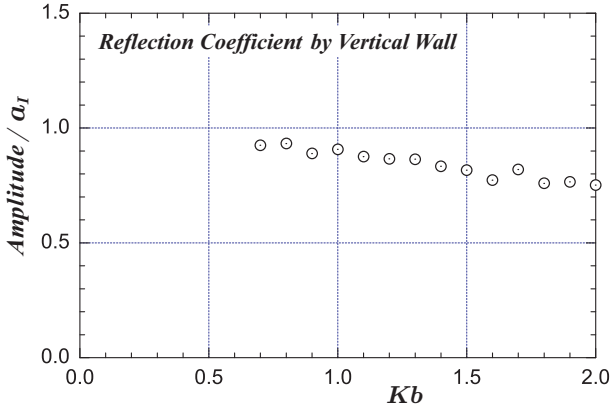

Fig. 5 Measured reflection-wave coefficient by a vertical wall, from which the wave attenuation factor was obtained at each frequency.

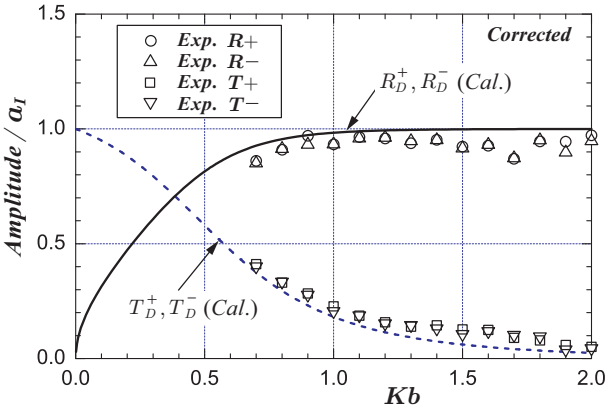

Fig. 6 Reflection and transmission coefficients for the diffraction problem (with correction for wave attenuation).